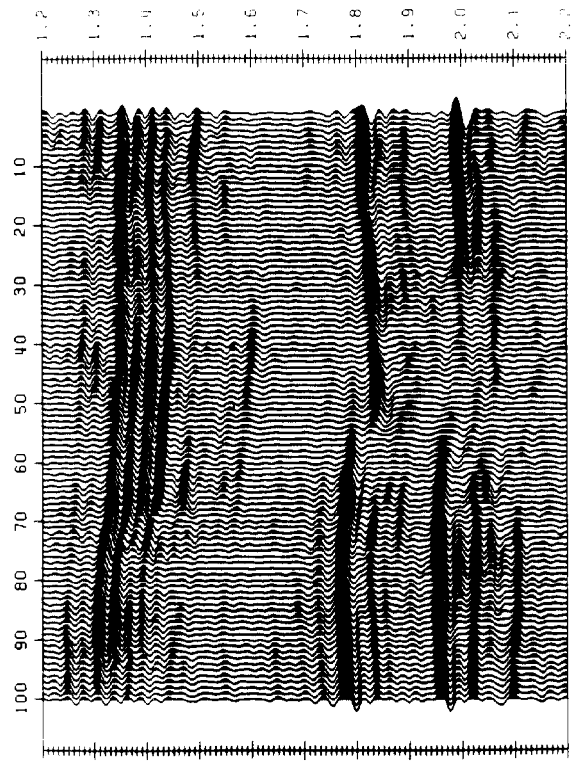

FIG. 3. Stacked section after zero-phase post-stack deconvolution.

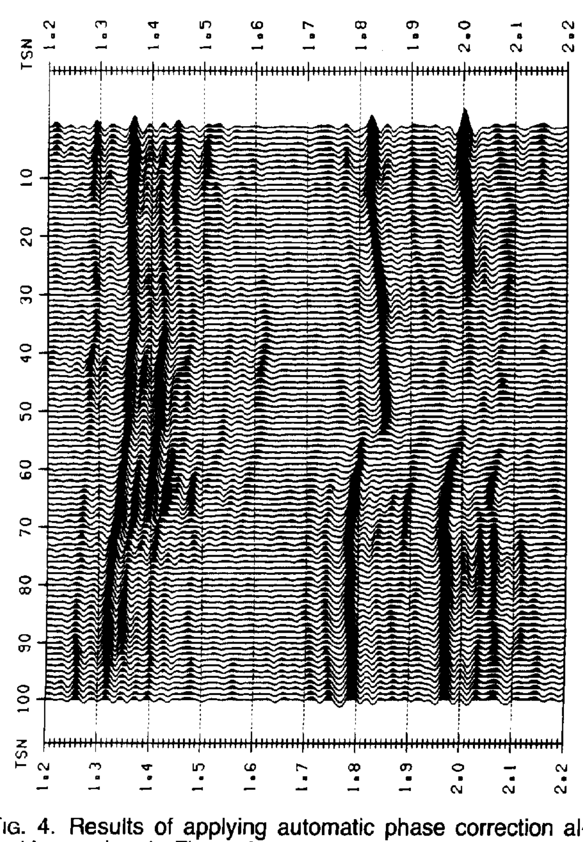

FIG. 4. Results of applying automatic phase correction algorithm to data in Figure 3.

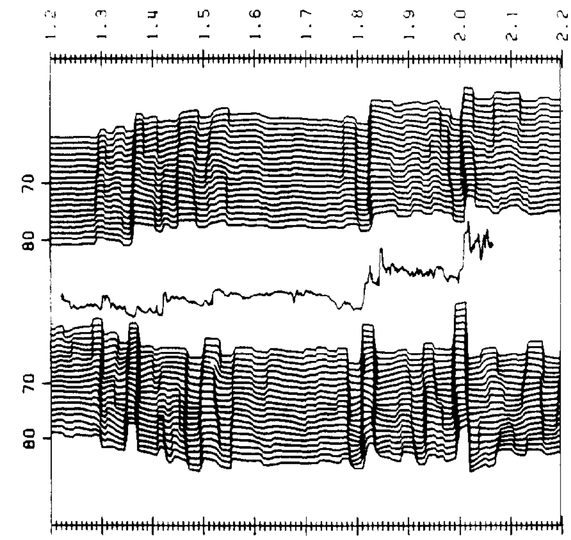

FIG. 5. Log relative impedances shown on left were obtained by inverting 20 seismograms near trace 80 in Figure 3. These results do not compare favorably with velocity log plotted in center of diagram. Log relative impedance obtained by inverting 20 of corresponding phase-corrected data in Figure 4 shown on right side of this figure. Improved match to well is obvious.

applied to the data sets in both Figures 3 and 4 and the results for 20 consecutive traces in the vicinity of well site are shown in Figure 5. The relative impedance traces to the right of the well log correspond to the phase-corrected data while those to the left correspond to the uncorrected data. Obviously, the application of the phase correction algorithm to these data resulted in an improved match between the well-log relative impedance and the calculated relative impedance functions. Furthermore, comparison of the faulted zone (traces 50 to 70, between 1.6 to 2.0 s) in Figures 3 and 4, shows a better fault definition on the phase-corrected output.

The two methods for determining the residual phase are complementary and we often apply both methods to data when a well log exists. In the majority of cases the phase shifts predicted by the two methods are in acceptable agreement.

References

Levy, S., and Oldenburg, D., 1982, The deconvolution of phase-shifted wavelets: Geophysics, **47**, 1285–1294.

Levy, S., and Fullagar, P. K., 1981, Reconstruction of a sparse spike train from a portion of its spectrum and application to high-resolution deconvolution: Geophysics, **46**, 1235–1243.

Oldenburg, D. W., Scheuer, T., and Levy, S., 1983, Recovery of the acoustic impedance from reflection seismograms: Geophysics, **48**, 1318–1337.

Wiggins, R. A., 1978, Minimum entropy deconvolution: Geoexpl., **16**, 21–35.

Stable Inversion of Zero-Offset Seismic Data S3.3

Børge Arntsen, Petroleum Technology Research Institute; and Bjørn Ursin, Seismic Research and Development A/S, Norway

In a previous paper it was shown that the zero-offset reflection response due to a point source from a stack of homogeneous layers of variable thickness can be used to compute the thickness, velocity, and density in each layer. However, the proposed scheme was found to be sensitive to noise in the data. A stable scheme is obtained by minimizing the sum of the squared differences between the data and the output from a modeling program. The model parameters (layer thickness, velocity, and density) are iteratively updated until the minimum is reached.

Numerical results obtained with synthetic data show that the method is limited to shallow seismic data. For large values of the geometrical spreading, only the acoustic impedance as a function of traveltime can be estimated. That is, the wavefront becomes almost planar, and the wave propagation is goverened by the one-dimensional wave equation.

Introduction

This paper presents a method for estimating wave velocities and densities as a function of depth in a horizontally layered medium. In a previous paper it was shown that the zero-offset reflection response due to a point source can be used to compute thickness, velocity, and density in each layer by a simple scheme. The scheme is, however, sensitive to noise, and we now propose to use a least-squares method. The method minimizes the sum of squared differences between the data and a synthetic response computed from a model. It was found earlier (Cook and Schneider, 1983; Bamberger et al., 1982) that such an inversion scheme is indeed stable.

Zero-offset modeling

The measured response in a seismic experiment may be related to the parameters describing the subsurface through a set of equations which we call the forward model. We consider vertically traveling waves in a horizontally layered elastic medium where each layer is characterized by the wave velocity c_k, density ρ_k, and thickness $D)_k$.

According to ray theory (Ursin and Arntsen, 1983), the displacement velocity at the receiver is given by a sum of terms corresponding to all primary and multiple reflections. Each term contributes an amount,

$$V(\boldsymbol{\theta}) = \prod_{i=1}^{k} H_i(\theta), \tag{1}$$

where $\boldsymbol{\theta}$ is a parameter vector defined as

$$\boldsymbol{\theta} = (C_1, \rho_1, D_1, \ldots, C_N, \rho_N, D_N),$$

and the first H factor is the source pulse shape delayed by the traveltime τ given by

$$\tau = \sum_{k=1}^{N} s_k D_k / C_k. \tag{3}$$

Here s_k is the number of times the ray has traversed layer k. The geometrical spreading is expressed by the second H factor as

$$H_2 = \left(\sum_{k=1}^{N} s_k \, C_k \, D_k \right)^{-1}. \tag{4}$$

The rest of the factors in equation (1) contain transmission and reflection coefficients.

To evaluate a realistic response, a large number of rays must be included in the calculations. We use an automatic ray-generation scheme which includes primary reflections and waves reflected up to a certain number of times. The resulting response vector is denoted by $\mathbf{f}(\boldsymbol{\theta})$ and has components

$$\mathbf{f}(\boldsymbol{\theta}) = (f_1, f_2, \ldots, f_L). \tag{5}$$

Component k is the response at time $\tau_k = k\Delta t$, Δt being a suitable sampling interval.

Least-squares inversion

The measured seismic data may now be described by the forward model

$$\mathbf{Y} = \mathbf{f}(\boldsymbol{\theta}), \tag{6}$$

where $\mathbf{Y}$ is the data vector. Assuming that second-order terms in a Taylor expansion of $\mathbf{f}$ may be neglected, we obtain

$$\Delta \mathbf{Y}_k = \mathbf{F}_k \Delta \boldsymbol{\theta}. \tag{7}$$

Here $\Delta \mathbf{Y}_k = \mathbf{Y} - \mathbf{F}(\hat{\boldsymbol{\theta}}_k)$, $\Delta \boldsymbol{\theta} = \boldsymbol{\theta} - \boldsymbol{\theta}_k$, and $\underset{\sim}{\mathbf{F}}_k$ is the Jacobian matrix whose elements are given by

$$F_{k,ij} = \frac{\partial f_i}{\partial \theta_j}, \tag{8}$$

evaluated at $\boldsymbol{\theta} = \hat{\boldsymbol{\theta}}_k$. $\boldsymbol{\theta}_k$ is the estimate of $\boldsymbol{\theta}$ in iteration k. The next estimate of $\boldsymbol{\theta}$ is $\hat{\boldsymbol{\theta}}_{k+1} = \hat{\boldsymbol{\theta}}_k + \Delta\hat{\boldsymbol{\theta}}_{k+1}$ which is found by solving the least-squares problem,

$$\min \| \Delta \mathbf{Y}_k - \underset{\sim}{\mathbf{F}}_k \Delta \boldsymbol{\theta} \|. \tag{9}$$

The solution is

$$\Delta \boldsymbol{\theta}_{k+1} = \hat{\underset{\sim}{\mathbf{S}}}^{-1} \Delta \mathbf{Y}_k,$$

where $\hat{\underset{\sim}{\mathbf{S}}}^{-1}$ is a generalized inverse of the matrix

$$\underset{\sim}{\mathbf{S}}_k = \underset{\sim}{\mathbf{F}}_k \Delta \boldsymbol{\theta}, \tag{10}$$

Table 1. Inverted model using synthetic data without noise.

Exact model			Initial model			Inverted model, no noise		
C (m/s)	D (m)	ρ (g/cm³)	C (m/s)	D (m)	ρ (g/cm³)	C (m/s)	D (m)	ρ (g/cm³)
0	–	0.00	0	–	0.00	0	–	0.00
1500	125	1.09	1500	125	1.09	1500	125	1.09
1615	119	1.46	1500	112	1.20	1611	119	1.46
2050	200	1.86	1500	146	1.40	2050	200	1.86
1950	250	1.77	1500	192	1.20	1950	250	1.77
2160	100	1.90	1500	69	1.80	2160	100	1.90
3050	150	2.20	1500	74	2.00	3051	150	2.20
3160	250	2.25	1500	119	2.10	3165	250	2.25
5350	260	2.57	1500	73	2.20	5349	260	2.57
3600	350	2.35	1500	146	2.00	3602	350	2.35
4700	–	2.47		–	2.47	4700	–	2.47

computed by a modified Marquardt-Levenberg algorithm (More, 1977).

Numerical results

Synthetic data were computed using the model defined in Table 1. An air gun source and the receiver were positioned just below the surface. Least-squares inversion was then applied to the synthetic trace with initial parameter values as given in Table 1. The parameters were chosen such that traveltimes for each layer were close to the traveltimes in the model used for generating the synthetic trace.

The results of the inversion using noise-free data, data with medium noise level, and data with high-noise level is shown in Tables 1–2 and Figures 1–3. The error in the estimated parameters increases with depth. This is partly due to the fact that for large values of geometrical spreading the wavefront becomes almost planar, and wave propagation is described by the 1-D wave equation. As is known, only acoustical impedance may be recovered in this case. Also the signal-to-noise ratio increases with traveltime, especially reducing the information contained in the multiple reflections from deep layers. This makes estimation of velocities, densities, and layer thicknesses difficult, and limits the method to shallow data. Acoustical impedance may, however, be estimated even for deep reflectors with relatively large S/N ratio.

Table 2. Inverted model using synthetic data with low and high noise level.

Inverted model, medium noise			Inverted model high noise		
C (m/s)	*D* (m)	ρ (g/cm³)	*C* (m/s)	*D* (m)	ρ (g/cm³)
0	–	0.00	0	–	0.00
1500	125	1.09	1500	125	1.09
1622	120	1.45	1795	133	1.30
2211	216	1.73	1986	194	2.02
1936	248	1.77	1870	240	1.92
2048	95	2.00	2718	127	1.50
4012	198	1.70	2401	121	3.00
2270	179	3.22	1941	151	4.05
4253	206	3.32	1977	96	7.11
2151	209	4.25	1829	177	5.52
4700	–	2.47	4700	–	2.47

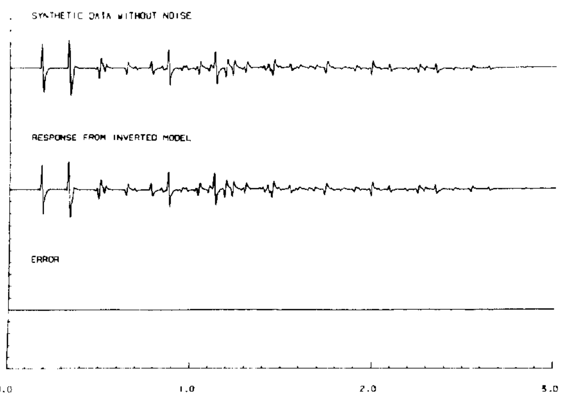

FIG. 1. Response from inverted model using synthetic data without noise.

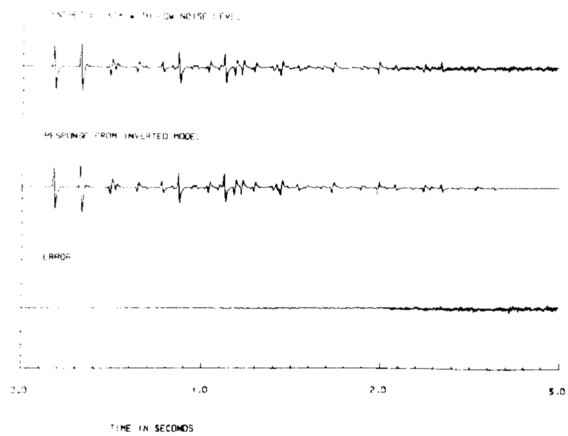

FIG. 2. Response from inverted model using synthetic data with low noise level.

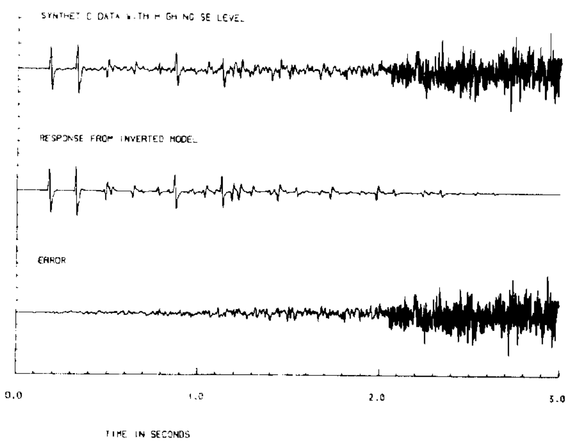

FIG. 3. Response from inverted model using synthetic data with high noise level.

References

Bamberger, A., Chavent, G., Hemon, Ch., and Lailly, P., 1982, Inversion of normal incidence seismograms: Geophysics, **47**, 757–770.

Cooke, D. A., and Schneider, W. A., 1983, Generalized linear inversion of reflection seismic data: Geophysics, **48**, 665–676.

More, 1977, The Levenberg-Marquardt algorithm: Implementation and theory, *in* Watson, G. A., Ed., ,Numerical analysis: Lecture notes in mathematics, Springer-Verlag.

Ursin, B., and Arntsen, B., 1985, Computation of zero-offset vertical seismic profiles including geometrical spreading and absorption: Geophys. Prosp., **33**, 72–96.

Robust Iterative Inversion for the One-Dimensional Acoustic Wave Equation S3.4

Adam Gersztenkorn, Amoco Production Co.; J. Bee Bednar, Amerada Hess Corp; and Larry R. Lines, Amoco Production Co.

The one-dimensional geophysical inverse problem is solved by considering a linearized integral equation which is deduced from the wave equation. This Born inversion approach is shown to be equivalent to linear least-squares inversion for a particular parameterization of the medium. The least-squares solution is also considered as a member of a family of generalized LP norm solutions which are deduced from a maximum likelihood formula-